PNAS Nexus, 2023, 2, 1–9
https://doi.org/10.1093/pnasnexus/pgad307
Advance access publication 19 September 2023
Research Report

The impact of current and future climates on spatiotemporal dynamics of influenza in a tropical setting

Ayesha S. Mahmud [a,*], Pamela P. Martinez [b,c] and Rachel E. Baker [d,e]

[a]Department of Demography, University of California, Berkeley, Berkeley, CA, USA
[b]Department of Microbiology, University of Illinois Urbana-Champaign, Champaign, IL, USA
[c]Department of Statistics, University of Illinois Urbana-Champaign, Champaign, IL, USA
[d]Department of Epidemiology, School of Public Health, Brown University, Providence, RI, USA
[e]Institute at Brown for Environment and Society, Brown University, Providence, RI, USA
*To whom correspondence should be addressed: Email: mahmuda@berkeley.edu
Edited By: Richard Stanton

Abstract

Although the drivers of influenza have been well studied in high-income settings in temperate regions, many open questions remain about the burden, seasonality, and drivers of influenza dynamics in the tropics. In temperate climates, the inverse relationship between specific humidity and transmission can explain much of the observed temporal and spatial patterns of influenza outbreaks. Yet, this relationship fails to explain seasonality, or lack there-of, in tropical and subtropical countries. Here, we analyzed eight years of influenza surveillance data from 12 locations in Bangladesh to quantify the role of climate in driving disease dynamics in a tropical setting with a distinct rainy season. We find strong evidence for a nonlinear bimodal relationship between specific humidity and influenza transmission in Bangladesh, with highest transmission occurring for relatively low and high specific humidity values. We simulated influenza burden under current and future climate in Bangladesh using a mathematical model with a bimodal relationship between humidity and transmission, and decreased transmission at very high temperatures, while accounting for changes in population immunity. The climate-driven mechanistic model can accurately capture both the temporal and spatial variation in influenza activity observed across Bangladesh, highlighting the usefulness of mechanistic models for low-income countries with inadequate surveillance. By using climate model projections, we also highlight the potential impact of climate change on influenza dynamics in the tropics and the public health consequences.

Keywords: influenza, mathematical modeling, climate, disease transmission

Significance Statement

Characterizing the seasonality of influenza—and the associated drivers—are crucial for control efforts in low-income countries. We quantified the role of climate in driving influenza dynamics in the tropics using data from Bangladesh. We documented annual peaks during the monsoons and a spatial gradient in the timing of peaks, which are well explained by a bimodal relationship between humidity and transmission. To our knowledge, this is the first study to identify the key drivers of these observed patterns, allowing us to quantify the possible effect of future climate on the transmission of influenza in Bangladesh. Our study demonstrates a unique approach for combining limited surveillance data with mathematical modeling, providing a framework for influenza forecasting in similar settings.

Introduction

Annual influenza outbreaks cause substantial mortality and morbidity globally. Influenza spreads person-to-person through respiratory droplets and aerosols, and exhibits a marked seasonal pattern in incidence and transmission in many populations. The role of climatic factors in driving the strong seasonal outbreak pattern of influenza outbreaks in temperate regions has been well studied (1–3). The dynamics of influenza in the tropics is less well characterized, with some countries experiencing annual peaks during the rainy season (4–7) and some experiencing year-round transmission (8–10). The paucity of data from countries in the tropics, along with the irregularity of observed seasonal patterns, has made it challenging to disentangle the relative importance of climatic drivers, demographic, and human behavioral factors, as well as changes in population immunity due to antigenic drift. As a result, relatively few studies have focused on modeling influenza dynamics and its driving factors in the tropics, despite the fact that influenza exerts a significant health burden in tropical regions (11). In low-income tropical countries, such as Bangladesh, the impact of the disease is likely compounded

Competing Interest: The authors declare no competing interest.
Received: December 5, 2022. **Revised:** July 25, 2023. **Accepted:** September 11, 2023

by malnutrition, lack of access to care, poor medical care, and the incidence of secondary bacterial infections (11, 12). Understanding and modeling influenza dynamics in these settings—where routine surveillance is limited or nonexistent—can provide better estimates of disease burden, improve seasonal forecasts, and aid in preparedness of the healthcare system.

Influenza outbreaks in temperate regions typically occur during the dry winter season (13). Laboratory studies have shown an inverse relationship between absolute or specific humidity (SH) and influenza virus survival and transmission potential (3, 14, 15). This corresponds well with the typical annual influenza peak observed in the winter months in temperate regions, when SH tends to be at lowest observed levels, and the very small number of cases observed in the summer months when SH is generally higher. In tropical and subtropical regions, the seasonal pattern appears to be less well defined; in countries that do experience seasonal outbreaks, the peak tends to occur during the hot, rainy season (4–7, 16) with an occasional peak during winter (7, 9). The typical inverse relationship between SH and influenza transmission, that has been used for modeling dynamics in temperate regions, fails to capture the pattern of influenza outbreaks in the tropics and subtropics, where SH is relatively high year-round and tends to peak during the rainy season. Previous work has suggested that a bimodal relationship between SH and influenza transmission might better explain the observed outbreak patterns in the tropics and subtropics (17–19), although this has only been demonstrated through mechanistic modeling for one city to date (19). Since the dynamics of recurrent outbreaks are also dependent on the continuous supply of susceptible individuals—added to the population through births and loss of immunity—mechanistic models are needed to account for the inherent nonlinear dynamics. This is especially true for influenza where infected individuals have immunity after they recover, but eventually become susceptible again because of continual antigenic drift of the influenza virus.

Here, we use eight years of influenza surveillance data from 12 districts in Bangladesh, to quantify the role of climatic factors in driving influenza dynamics. We adapt a mechanistic influenza model (19) that allows for high transmission at both low and high levels of SH, and decreased transmission at very high temperatures. We estimate the relationship between influenza transmission and climatic drivers, while accounting for changes in population immunity. We find that the best-fit model can accurately capture both the temporal and spatial variation in influenza activity observed across Bangladesh over several years, highlighting the usefulness of mechanistic models for low-income countries with inadequate surveillance. Finally, we use the modeled relationship between influenza transmission and climatic drivers to highlight the potential impact of climate change on influenza dynamics in tropical settings with a distinct rainy season.

Results

For each sentinel site, we calculated the test-positivity rate for influenza for each month, i.e. the proportion of samples tested that are positive for influenza. The test-positivity measure closely tracks the number of total influenza cases detected in the sentinel surveillance system (online supplementary Fig. S1), and can be compared across sites and over time as it is normalized by the number of samples tested.

All districts in Bangladesh, included in our study, experienced annual outbreaks of influenza with clear peaks and troughs rather than year-round transmission. Influenza activity in Bangladesh peaks in May during the monsoon season, which is characterized by high levels of precipitation, high SH, and a narrow temperature range from around 26 to 30°C (Figs. 1 and 2D). Influenza activity can also be high during the premonsoon season, but typically only when the SH is very high (above 14 g/kg) or very low (below 11 g/kg). Influenza activity is typically low during the winter months when both SH and temperature are at their lowest observed values. In general, high levels of influenza circulation in Bangladesh coincides with relatively high SH (above 14 g/kg), but within a narrow temperature range around 28°C.

We first used a multivariate logistic regression model to understand the relative impact of the climate predictors on influenza activity. We examined the univariate relationship of each climate variable—SH, temperature, and precipitation—with influenza activity. We also fit a multivariate model that includes all three predictors, which provides a better fit to the data than the univariate models (lowest AIC, see online supplementary Table S1). We find that when all three climate variables are included in the model, there is no significant effect of either temperature or precipitation. Our estimated effect size for temperature was similar in magnitude to the estimated effect size for SH (online supplementary Table S1)—and showed an inverse relationship between temperature and transmission at high temperatures (Fig. 2B), in line with existing literature (5, 18, 19). The imprecision in our estimated coefficient for temperature, and the resulting large confidence intervals, may be due to collinearity between temperature and specific humidity (18).

We find strong evidence for a nonlinear impact of SH on influenza test-positivity, with highest positivity rates observed for relatively low and high SH values (Fig. 2A). The coefficients on SH (OR: 0.46, 95% CI: 0.31–0.68) and SH^2 (OR: 1.03, 95% CI: 1.02–1.05) were statistically significant ($P < 2.2 \times 10^{-16}$) under a joint hypothesis test with heteroskedasticity-robust standard errors. Our regression model includes month and sentinel site fixed-effects dummy variables which allows us to estimate the effect of interannual variation in climate conditions while controlling for possible unobserved confounders that vary across sites or seasonally. Overall, these results suggest that SH is an important driver of influenza activity in Bangladesh, with peak activity occurring at both low and high levels of SH.

To further confirm the hypothesis that SH is a fundamental driver of influenza seasonality and interannual variability in Bangladesh, and to estimate influenza burden under current and projected climates, we examined whether a mechanistic model of disease transmission with climate covariates could reproduce the national and district-level seasonal pattern in observed test-positivity rates and the spatial variation in the timing of influenza peaks in Bangladesh. We fit a susceptible-infected-recovered-susceptible model (SIRS), which has been used previously to study influenza seasonality in the tropics and subtropics (19), to the observed time-series data on influenza seasonality. We modeled transmission as a bimodal function of daily SH, as is evident from our regression results. Although the estimated effect of temperature was not statistically significant in our regression, we include a temperature effect in the mechanistic model since the estimated temperature profile is closely aligned with findings from lab-based studies that have shown that influenza virus survival decreases as temperature increases (20). Prior research has also shown that mechanistic models that include both SH and temperature as drivers of transmission significantly outperform models with transmission driven by humidity alone (19). We fit the model to data from January 2012 to December 2017 for each site and generate

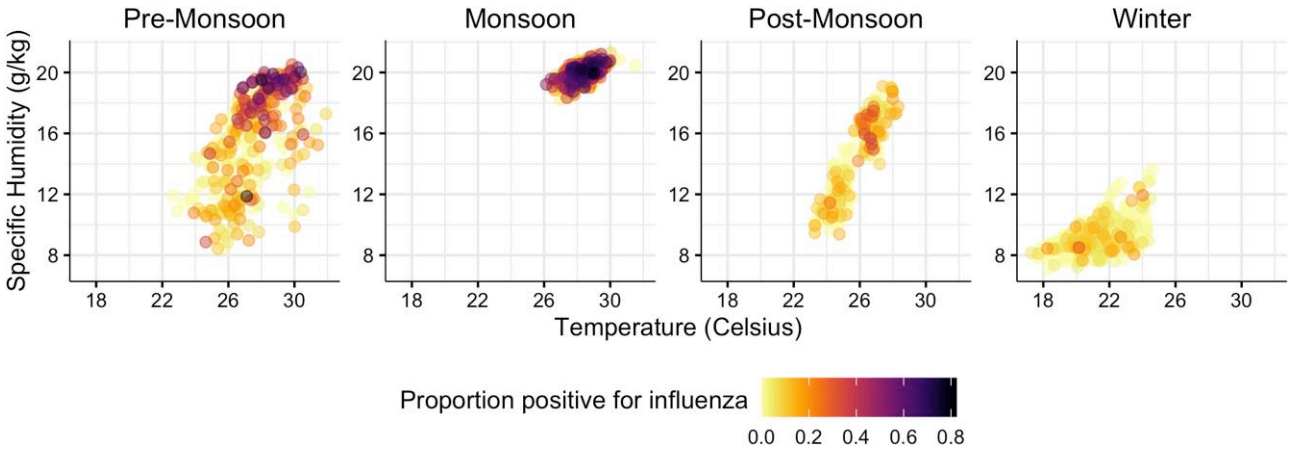

Fig. 1. Test-positivity rate (proportion positive) for influenza by season and climate conditions (temperature and specific humidity).

out-of-sample predictions for two years (January 2018 to December 2019).

The best-fit parameter estimates from the fitted model for each district produced consistent estimated effects for SH and temperature on influenza activity (online supplementary Fig. S2). We are able to reproduce the general year-to-year pattern in influenza incidence at the district level (Fig. 3), as well as the overall seasonality of influenza activity in Bangladesh (Fig. 4A). Further, the simulations also capture longitudinal and latitudinal gradients in influenza outbreak timing observed in Bangladesh (Fig. 4B and C). In Bangladesh, influenza exhibits a spatial pattern where outbreaks start earlier in the south and southeast of the country (Fig. 4B and C) and peaks the latest in the west. We also noted that influenza tends to peak earliest in the capital city Dhaka in the sentinel surveillance data, similar to previous findings (21, 22). The observed spatial gradient is accurately captured in our simulated incidence, although with a slight lag in the center of gravity of outbreaks (Fig. 4B and C). The lag between the simulated and observed data may be due to reporting delays. Detected cases are unlikely to be documented at onset of symptoms and patients may show up in the surveillance system days or weeks after symptoms onset (23), thereby leading to a bias in the data. Another possible reason for the discrepancy is differences in the shape of the outbreak curve between the simulated and observed data. The center of gravity measure captures the mean-weighted distribution of cases across the year. In general, we find that the simulated outbreaks have sharper peaks and are less diffuse than the observed data, which could be due to factors that are not accounted for in our model such as population density, contact patterns and mobility (24). Nonetheless, we are able to capture the overall seasonality, as well as the gradient in seasonality.

We also compared the simulations from the climate-driven model to two alternate models without climate—a null model with constant transmission year-round and a model with sinusoidal seasonal forcing. The best-fit null model simulations exhibited year-round circulation with no seasonal peaks, and with annual variations driven entirely by changes in the susceptible population. The climate-driven model vastly outperformed the null model for all districts (average RMSE of 0.558 for null model versus 0.228 for the climate model) and also outperformed the model with sinusoidal forcing (average RMSE of 0.243 for the sinusoidal model). In 5 out of 12 districts, the sinusoidal model outperformed the climate model for the test period. However, sinusoidal forcing leads to periodic uniform outbreaks, and the model is incapable of capturing any year-to-year variability seen in the real data (online supplementary Figs. S9 and S10). This is also reflected in lower RMSE values for the climate-driven model in all districts during the training periods (online supplementary Fig. S8). In general, our results show that a model that accounts for climate explicitly is better able to capture the spatiotemporal dynamics of influenza in Bangladesh.

Our fitted parameter estimates provide useful and novel insight into influenza dynamics and transmission in Bangladesh. We estimated the influenza reproduction number (R_0) in Bangladesh to be around 2 (HDI: 1.84–2.52), based on the overall best-fit parameters and the average SH and temperature across Bangladesh over the observation time period. We also estimated a duration of immunity (L) of just over a year (HDI: 365.24–727.01 days) and a duration of infection (D) of 3.8 days (HDI: 2.36–4.08 days). In our model, the lowest R_0 values occur at SH of 11 g/kg (HDI: 4.00–11.33 g/kg); transmission increases until SH reaches 19.6 g/kg (HDI: 17.07–19.91 g/kg) before leveling off; transmission increases as SH decreases from 11 to 3 g/kg (HDI: 2.30–34.00 g/kg) before leveling off (see online supplementary Table S2 and Fig. S6). Our estimated bimodal relationship between SH and transmission is strikingly similar to previous work looking at the relationship between SH and the probability of influenza peaks across multiple sites (17), as well as estimates using the same model in Hong Kong (19). Our estimates for the effect of temperature on transmission are also consistent with previous estimates suggesting a maximum temperature threshold beyond which transmission decreases with increasing temperature (18, 19, 25). We estimate this turning point (T_c) to be around 23.2°C (HDI: 21.36–29.95°C).

Finally, we use the best-fit model parameters to simulate influenza dynamics under current and predicted future climate conditions in Bangladesh. According to the most recent projection data from the Coupled Model Intercomparison Project Phase 6 (CMIP6) Shared Socioeconomic Pathway scenario 3 and the Representative Concentration Pathway 7.0 (SSP3-7.0), both SH and temperature are expected to increase in Bangladesh throughout the year, particularly during the monsoon and postmonsoon months (Fig. 5A and B). Our simulations reveal interesting variations in the impact of climate change across the country. Interestingly, all districts in our study experience a small decline in overall burden under projected climate, largely due to monsoon and postmonsoon

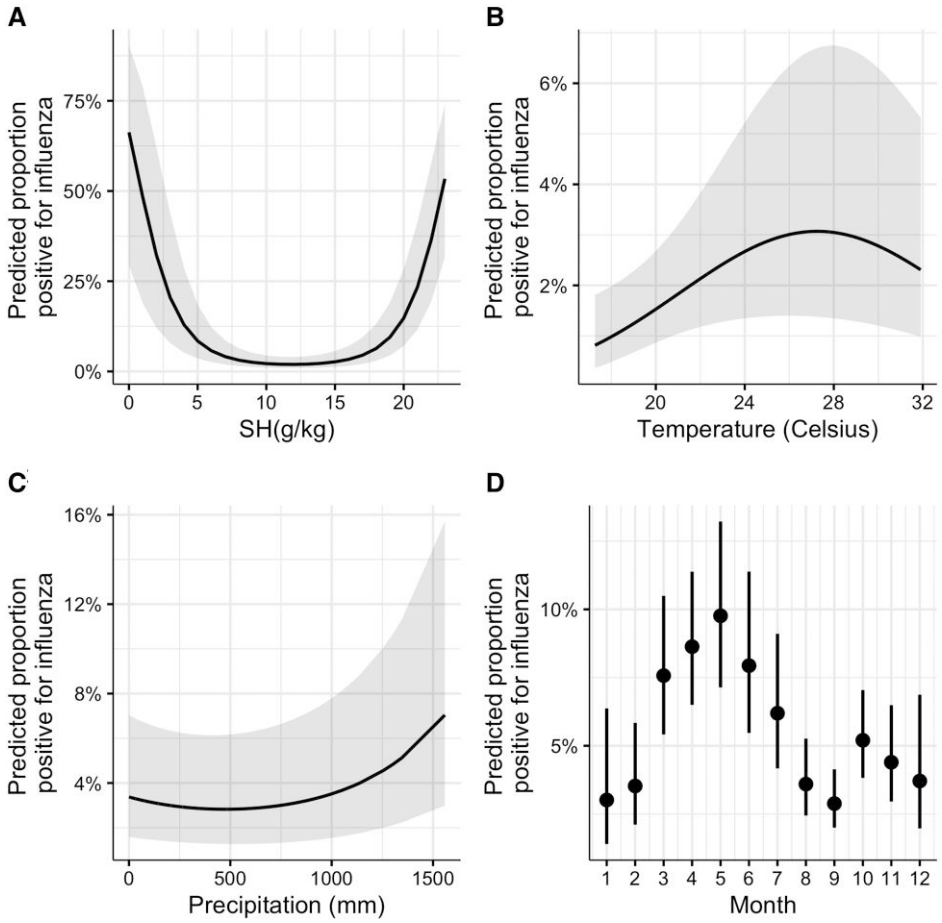

Fig. 2. Marginal effects plot showing the predicted proportion positive for influenza, and the associated 95% confidence intervals, by A) specific humidity; B) temperature; C) precipitation; and D) month. Predictions come from a multivariate logistic regression model fit to observed proportion of tests that are positive for influenza. The model also includes sentinel site fixed effect dummy variables. The marginal effects plot shows the predicted proportion positive for influenza for each variable, while holding all other variables constant (the constant values for the variables are temperature = 26.06°C; SH = 15.57 g/kg; precipitation = 190.92 mm; month = January; Hospital = Barisal).

temperatures far exceeding our estimated temperature threshold beyond which transmission is reduced. While winter months are projected to experience temperature ranges that are more favorable for transmission in the future, the increase in SH to the low transmission range dampens any favorable effect of temperature increases in the wintertime. While the overall burden is projected to decline, the peak incidence is projected to increase sharply in several districts in the east of the country, including Mymensingh and Sylhet, the fourth and fifth largest districts, respectively, by population size. This sharp increase in the peak is likely driven by two factors—(1) increased transmission during the monsoon season due to projected increases in SH and (2) reduced transmission during the winter months (due to SH falling in the low transmission range) allowing susceptible individuals to build up more quickly for a larger monsoon outbreak.

Discussion

Although the environmental drivers of influenza have been well studied in high-income settings in temperate regions, many open questions remain about the burden, seasonality, and drivers of influenza dynamics in the tropics. Consistent with previous studies from Bangladesh (21, 22, 26), we document annual seasonal peaks during the monsoons and a spatial gradient in the timing of peaks. The novel contributions of our study are to identify key drivers of these observed patterns that have remained a puzzle in the literature to date, and to disentangle the effect of future climate conditions on the transmission of influenza in Bangladesh.

Our mechanistic climate-driven model—which outperformed models with no climate-drivers—is able to explain the spatial and temporal dynamics across 12 districts in Bangladesh, and provides a framework for estimating current and future burden of influenza in tropical settings. Our estimated impact of SH on influenza transmission is strikingly similar to findings from Hong Kong (19), and provides further evidence for the hypothesis that a bimodal relationship between SH and transmission is needed to explain the pattern of influenza outbreaks in the tropics.

We use this estimated relationship to project influenza dynamics under future projected changes in climate. Overall, our results suggest that extremely high temperatures may dampen the impact of increased SH on transmission in the future, although this effect appears to be spatially heterogeneous. While we project an overall decline in annual influenza burden under future climate conditions, we find that several highly populated districts experience a sharp increase in peak incidence as outbreaks become more concentrated in the monsoon months. This suggests an increased need for healthcare resources during peak influenza season in Bangladesh in the future.

Our study has several limitations. First, we rely on sentinel surveillance data which does not allow us to calculate incidence

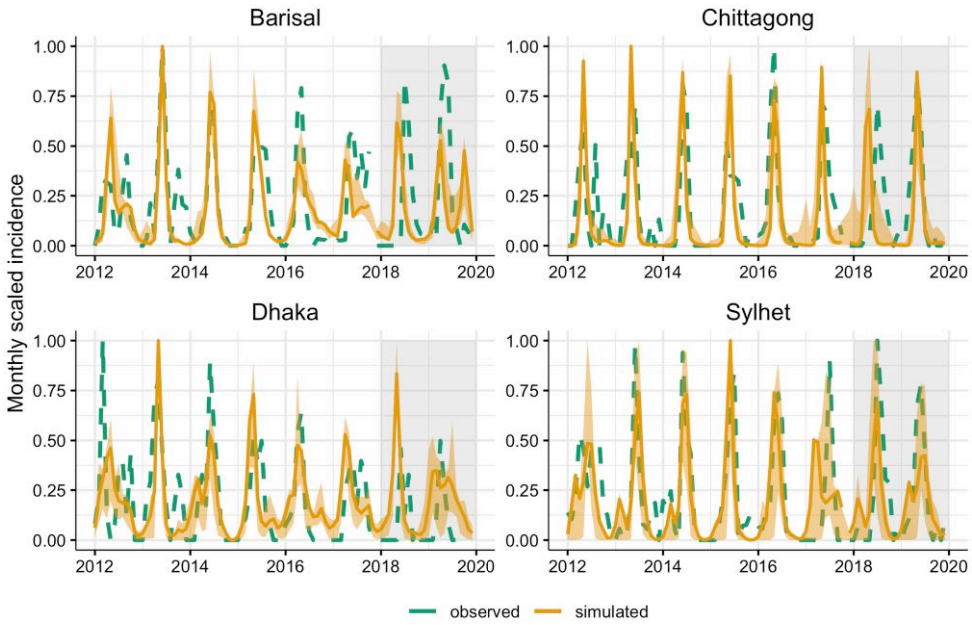

Fig. 3. Observed and simulated monthly incidence (scaled to be between 0 and 1) for four districts in Bangladesh. Green dashed line shows the observed monthly data; yellow solid line shows the best-fit simulation for each district based on the RMSE; yellow shaded area shows the range of simulated incidence for the top 10 best-fit simulations for each district. The model was fit to data from 2012 to 2018 (training period). The gray shaded region shows the testing period from 2018 to 2020. Online supplementary Fig. S3 shows results for all 12 districts.

directly, and may not accurately reflect the overall dynamics of influenza at the district level. The system is more likely to capture the more severe influenza cases, and is subject to reporting delays. The test-positivity measure may also be biased, and may not accurately reflect the spatiotemporal pattern of influenza incidence. Nonetheless, the observed pattern in our test-positivity measure is consistent with the strong seasonal and spatial dynamics that have been documented previously for Bangladesh (21, 22). Additionally, in settings where both test-positivity and other measures of influenza burden are available, the temporal dynamics of the test-positivity measure closely matches the temporal dynamics of other measures such as the number of hospitalized cases (27, 28).

A second limitation is that we use aggregated case data across all influenza subtypes. This impacts the estimation of the duration of immunity parameter and its interpretation. When there are multiple influenza strains circulating, recovered individuals may gain immunity against a particular subtype but remain susceptible to the other influenza subtypes either during the same or subsequent outbreak. We aimed to partially address this effect by incorporating waning immunity following antigenic drift, and thus, allowing individuals to re-enter the susceptible class at a defined rate. However, since we do not distinguish between influenza subtypes, the estimated duration of immunity is relatively short (HDI: 365.05–551.39 days). In essence, a shorter immunity period approximates the co-circulation of influenza virus subtypes and allows the simulations to capture the frequent outbreaks observed in Bangladesh. This makes the parameter difficult to interpret, but previous work suggests that this does not affect model performance (19). Additionally, aggregating all cases may mask interactions among subtypes that could play a role in modifying the association of influenza with climatic drivers (29). Expanding the model to include multi-strain dynamics is a important direction for future research.

A third limitation of our study is that we model each district separately without consideration for population mobility and contact patterns. Previous work has suggested that population mobility and seasonal changes in mobility and behavior can be an important drivers of the spatial spread of diseases in Bangladesh, including influenza (30, 31). Without additional data, we cannot fully rule out the possibility that seasonal forcing of influenza in Bangladesh is driven by additional extrinsic factors such as changes in host behavior. For respiratory pathogens, the opening and closing of schools has been shown to be an important driver of transmission seasonality (32); however, school term-time forcing is unlikely to explain the pattern of influenza transmission observed in Bangladesh, where transmission peaks during summer when schools are typically closed. Incorporating seasonal human mobility and contact behavior into metapopulation models for influenza transmission is an important avenue for future research.

Finally, this study only examines influenza dynamics in the period before the COVID-19 pandemic. The introduction of nonpharmaceutical interventions during the pandemic disrupted influenza transmission globally; this can serve as a useful natural experiment for disentangling the relative importance of environmental drivers, human behavior, and population immunity, and should be a key focus of future research efforts.

Characterizing the seasonality of influenza—and the associated drivers—is crucial for control and prevention efforts, for ensuring adequate preparedness of the medical system, and for determining the timing of vaccination campaigns. This is especially important for LMICs in tropical and subtropical settings, where public health resources are limited, surveillance may be poor or absent, and seasonality and burden have not been well studied. Our study demonstrates a unique approach for combining limited sentinel surveillance data with careful mechanistic modeling, and provides a framework that can be adapted for influenza forecasting in similar settings.

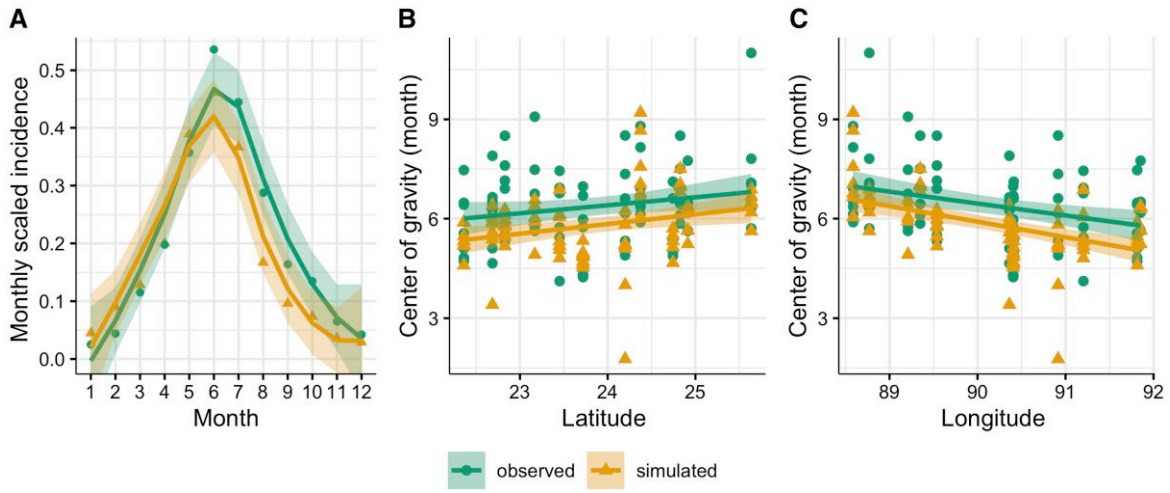

Fig. 4. Comparison of observed and simulated spatiotemporal trends in influenza activity. A) Seasonality in incidence, B) center of gravity for outbreaks by latitude, and C) longitude.

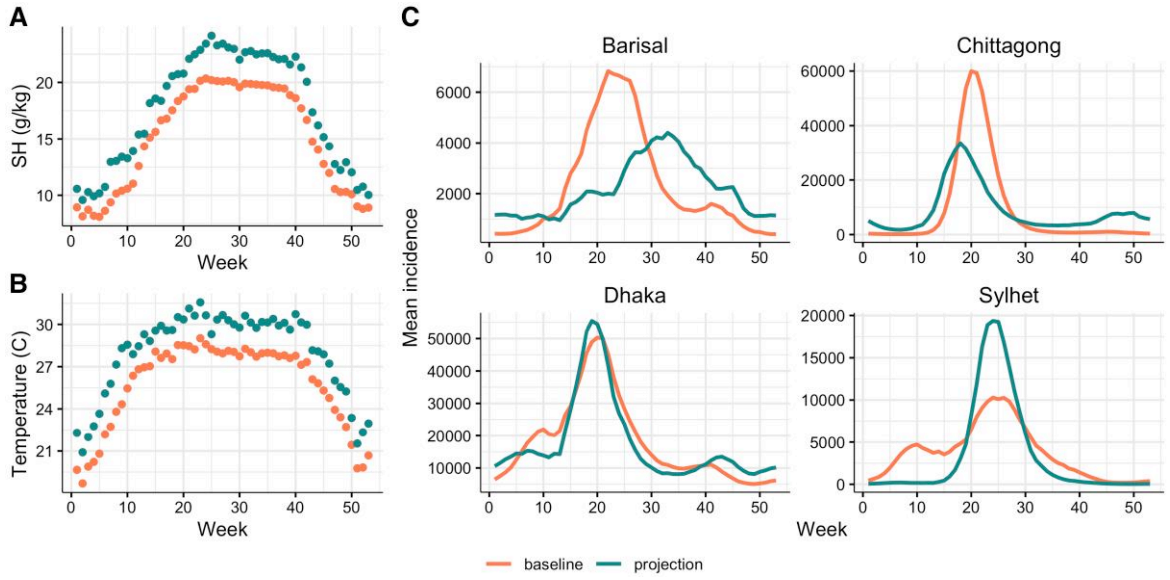

Fig. 5. Projected change in A) specific humidity and B) temperature averaged across all sentinel sites by week of year between baseline period and projection period (2085–2100). C) Comparison of simulated incidence with baseline climate versus projected climate (2085–2100) for four districts in Bangladesh. For each district, the mean incidence by week of year is shown. Online supplementary Fig. S5 shows results for all 12 districts.

Methods

Data

Influenza surveillance data

We used influenza data from two sentinel surveillance systems in Bangladesh: (1) the national influenza surveillance system (NISB) and (2) the hospital-based influenza surveillance system (HISB). Since 2010, 32 hospitals have participated in the surveillance program. Here, we use publicly available data for 19 hospitals from January 2012 to December 2019, spanning 18 districts (of 64 total) across Bangladesh. At each sentinel hospital site, on two randomly chosen days each week, nasal swabs were collected from patients with influenza-like illness (fever ≥38°C and cough within the last 10 days) from outpatient departments and patients with severe acute respiratory infection (fever ≥38°C and cough within the last 10 days and requiring hospitalization) from inpatient departments (22). Samples were tested by real-time RT-PCR to detect influenza. The publicly available data are aggregated at the monthly level for each site, and include the number of positive influenza cases as well as the number of samples tested. Since the number of influenza positive cases depend on the number of samples tested, which can vary by month and location, we use the test-positivity rate as a normalized measure for comparing influenza activity across time and space. We calculated the test-positivity rate for influenza for each month as the proportion of samples tested that are positive for influenza. The test-positivity measure closely tracks the influenza positive cases over time (online supplementary Fig. S1). We excluded data for 2020 and 2021 to avoid possible confounding due to the unusually low influenza activity over the course of the COVID-19 pandemic (33).

Climate data

We obtained data on temperature and specific humidity from the ERA5 gridded hourly dataset that combines model data with observations from across the world into a globally complete and

consistent dataset (34). We matched the gridded climate data to the hospital sentinel sites based on the latitude and longitude for each site. We averaged over the hourly observations to obtain monthly mean values for the temperature and specific humidity. We obtained precipitation data from the Climate Research Unit (CRU) gridded monthly dataset (35), and matched it to each sentinel site based on the site's coordinates.

We also obtained projected specific humidity and temperature data from the CMIP6, using the Geophysical Fluid Dynamics Laboratory (GFDL) model, under the Shared Socioeconomic Pathway scenario 3 and the Representative Concentration Pathway 7.0 (SSP3-7.0) (36). This scenario represents a middle-of-the-road outcome in terms of emissions trends and warming. This data is available in gridded format, and grid cells were matched to sentinel sites based on the latitude and longitude for each site.

Multivariate regression

To quantify the relationship between influenza seasonality and climate, we used multivariate logistic regression models. In order to account for a possible nonlinear relationship between influenza incidence and climate variables, we used second-degree polynomial functions for each of the climate predictors. We also included month and hospital site fixed-effects (dummy variables) to account for unobserved confounders. The dependent variable was the observed proportion of sampled cases that tested positive for influenza for each month and site from January 2012 to December 2019.

Mechanistic model with climate

Since the dynamics of infectious diseases are dependent on the supply of susceptible individuals and population-level immunity, mechanistic models are needed to account for the inherent nonlinear dynamics. We adapted the SIRS model from Ref. (19) that has been used previously to study influenza seasonality in Hong Kong, a large, dense city with subtropical climate. The SIRS model is as follows:

$$\frac{dS}{dt} = \frac{N - S - I}{L} - \frac{\beta(t) I^{\alpha} S}{N} + \mu(N - S), \tag{1}$$

$$\frac{dI}{dt} = \frac{\beta(t) I^{\alpha} S}{N} - \frac{I}{D} - \mu I, \tag{2}$$

where I is the number of infected individuals, S is the number of susceptibles, N is the size of the population, and $(N - S - I)$ is the size of the recovered population. The daily transmission rate is $\beta(t)$, which varies daily depending on the climatic conditions (as described below); D is the mean infectious period; L is the average duration of immunity; and α is an exponent on the number infected to account for the discretization of a continuous-time process and for imperfect population mixing (37). We set the birth rate and the death rate, μ, to be equal to maintain a constant population size; μ is set at 18 per 1,000 based on most recent data on the birth rate in Bangladesh.

The basic reproduction number at time t, $R_0(t)$, is equal to $\beta(t)D$ and is modeled as a function of the daily specific humidity, $q(t)$, and temperature, $T(t)$, as follows:

$$R_0(t) = [aq^2(t) + bq(t) + c]\left[\frac{T_c}{T(t)}\right]^{T_{exp}}. \tag{3}$$

Similar to Ref. (19), we used three parameters to describe and estimate the bimodal relationship between daily SH and R_0. This parabolic relationship is also consistent with the results of our multivariate regression. The parameter q_{mid} signifies the turning point for the parabola linking SH and R_0. As SH decreases from q_{mid} to q_{min}, R_0 increases before leveling off for SH values below q_{min}; conversely, as SH increases from q_{mid} to q_{max}, R_0 increases before leveling off at SH values above q_{max}. The parameters a, b, and c are defined as follows (see Ref. (19) for the full derivation):

$$a = \frac{-b}{q_{max} + q_{min}}, \tag{4}$$

$$b = \frac{(R_{0,max} - (R_{0,max} - R_{0,diff}))(q_{max} + q_{min})}{(q_{max} - q_{mid})(q_{min} - q_{mid})}, \tag{5}$$

$$c = (R_{0,max} - R_{0,diff}) - aq_{mid}^2 - bq_{mid}, \tag{6}$$

where $R_{0,max}$ is the maximum possible value of R_0 when SH is at q_{min} or q_{max} and temperature is at T_c; $R_{0,diff}$ is the difference between $R_{0,max}$ and the value of R_0 at the minimum point q_{mid}.

In our model, daily temperature, $T(t)$, modifies the impact of SH on R_0. Two parameters describe this relationship. T_c is the temperature threshold below which changes in temperature have no effect on transmission (as is the case in our multivariate regression results), while temperatures above T_c reduce transmission. The parameter T_{exp} determines the strength of the relationship between temperature and R_0 with higher values of T_{exp} indicating a sharper decline in R_0 with increasing temperatures above T_c.

Based on this model and the observed values for specific humidity and temperature, we simulated influenza incidence in each district deterministically in discrete daily time steps, and used the Runge–Kutta method for obtaining approximate solutions to the differential equations (Eqs. 1 and 2). We estimated the model parameters by fitting the simulations to the epidemiological data, as described below.

Best-fit parameter estimates

We estimated the "best-fit" model parameters by testing a wide range of parameter values, and tuning the parameter ranges against the observed influenza data. We split our observed data into a training period (January 2012–December 2017) for model optimization, and a testing period (January 2018–December 2019) for cross-validation. We included only districts that had at least 5 years of complete training data (12 out of the original 18 districts in the dataset). We chose 5,000 parameter combinations using latin hypercube sampling (LHS) based on parameter ranges from the literature (see online supplementary Table S2). We ran 5,000 simulations for each district based on these parameter combinations for the training period. For each simulation run, we had a burn-in period of 20 years (with average temperature and SH values) to allow the simulations to work through transient dynamics.

We assessed model fit based on how well the simulations matched observed influenza data for the training period. To allow for a comparison between simulated incidence data and observed test-positivity rates, we normalized the observed monthly test-positivity values to be between 0 and 1 over the entire observation period. We aggregated the simulated daily incidence to obtain monthly counts of new influenza cases, and normalized these counts to be between 0 and 1 over the entire observation period. This allows us to compare the simulation results with test-positivity data in the absence of observed incidence data. Thus, model fit is assessed on how well the model is able to capture seasonal and long-term trends in relative influenza incidence rather than the absolute number of influenza cases. We assessed model fit by calculating the root mean squared error (RMSE) between the normalized observed and simulated monthly values for each site.

We used an iterative process for obtaining parameter estimates. For each district, we chose the 500 parameter combinations (out of 5,000) with the lowest RMSE, and computed the 95% highest density interval (HDI) for each parameter. We used the 95% HDI to generate new parameter ranges if the 95% HDI upper (lower) bound was not within 10% of the original parameter range maximum (minimum) value. We re-generated 5,000 parameter combinations using LHS with the new set of parameter ranges, and repeated simulations for each district. We then repeated the steps for computing the 95% HDI described above. After six rounds of tuning, we found that parameter ranges did not shrink further and were within 10% of the HDI bounds. From the final parameter ranges, we generated 10,000 parameter combinations using LHS, and report results for the "best-fit" model by showing simulations for the 10 parameter combinations with the lowest RMSE for each district.

We also searched the parameter space for the best-fit model overall, across all districts. We report parameter estimates from the overall best-fit model, along with the 95% HDI interval for the the 500 parameter combinations (out of 10,000) with the lowest RMSE overall (summed across all districts). If SH and temperature are drivers of influenza seasonality in Bangladesh, we expect the model to capture overall seasonality in Bangladesh and district-level seasonal patterns. To look at the seasonality of influenza, we calculated the center of gravity of the monthly distribution of cases for both observed and simulated data for each district. We defined the center of gravity as the mean month of the distribution, where each month is weighted by its number of cases.

We also expect the best-fit simulations for each district to produce similar values for the effect of SH and temperature, as well as other parameter estimates. Finally, we expect the simulations to capture the overall spatial trend in the peak timing of influenza across Bangladesh, although this may be confounded by other causal processes such as population mobility patterns. We compared simulation results to observed data as a test of each of these hypotheses.

Alternate models without climate

We also compared our main model results with two alternate models that did not explicitly include climate: (1) a null model with constant transmission and (2) a model with sinusoidal forcing in transmission. For both models, we fit model simulations to the observed data using the same procedure described above, to estimate the best-fit model parameters. For the null model, we estimate the best-fit R_0 that is constant over time; for the sinusoidal forced model ($R_0(t) = \bar{R}_0(1 + \lambda \sin(\frac{2\pi}{365}(t + 270))$), we estimate the average annual reproduction number, $\bar{R}_0$ and λ, a parameter that controls the amplitude of the seasonal forcing relative to $\bar{R}_0$. The sinusoidal forcing function peaks in the middle of the year, which mimics the peak in annual influenza burden (online supplementary Fig. S7). For each alternate model, we calculated the RMSE (as described above) for each district.

Projections under climate change

We bias corrected the CMIP6 projection data by calculating the difference between the mean daily 2085–2100 temperature and SH and the mean daily 2005–2020 temperature and SH from the climate model output. We then applied this difference to our ERA5 observations for each sentinel site. We ran the influenza model using the baseline (ERA5) observed temperature and SH and the projected temperature and SH data for 8 years (the length of the influenza time series) and compared average daily cases in the current and future scenario. We also calculated the total average annual incidence (area under the curve) and peak incidence in both current and future scenarios.

Acknowledgments

We acknowledge the efforts and contribution of the influenza surveillance teams across Bangladesh. This manuscript is based on data collected and shared by the Institute of Epidemiology Disease Control and Research. We are grateful to Yuan et al. (19) for sharing their model code publicly.

Supplementary material

Supplementary material is available at *PNAS Nexus* online.

Funding

The authors declare no funding.

Author contributions

A.S.M. conceived and designed the study; collected, collated, and analyzed the data and wrote the first draft of the manuscript. All authors had access to the data, contributed to the interpretation of results, finalized tables and figures, critically reviewed and edited the manuscript, and approved the final version.

Data availability

All data are publicly available from the Institute of Epidemiology, Disease Control and Research, Bangladesh, and can be downloaded from here. All code for replicating the analysis is publicly available here on Github.

References

1 Shaman J, Pitzer VE, Viboud C, Grenfell BT, Lipsitch M. 2010. Absolute humidity and the seasonal onset of influenza in the continental United States. *PLoS Biol*. 8(2):e1000316.
2 Yang W, Lipsitch M, Shaman J. 2015. Inference of seasonal and pandemic influenza transmission dynamics. *Proc Natl Acad Sci USA*. 112(9):2723–2728.
3 Shaman J, Kohn M. 2009. Absolute humidity modulates influenza survival, transmission, and seasonality. *Proc Natl Acad Sci USA*. 106(9):3243–3248. doi:10.1073/pnas.0806852106
4 Tamerius JD, *et al*. 2013. Environmental predictors of seasonal influenza epidemics across temperate and tropical climates. *PLoS Pathog*. 9(3):e1003194.
5 Tamerius J, *et al*. 2010. Global influenza seasonality: reconciling patterns across temperate and tropical regions. *Environ Health Perspect*. 119(4):439–445.
6 Cummings MJ, *et al*. 2016. Epidemiologic and spatiotemporal characterization of influenza and severe acute respiratory infection in Uganda, 2010–2015. *Ann Am Thorac Soc*. 13(12):2159–2168. doi:10.1513/AnnalsATS.201607-561OC
7 Suntronwong N, *et al*. 2020. Climate factors influence seasonal influenza activity in Bangkok, Thailand. *PLoS ONE*. 15(9): e0239729. doi:10.1371/journal.pone.0239729
8 Viboud C, Alonso WJ, Simonsen L. 2006. Influenza in tropical regions. *PLoS Med*. 3(4):e89.

9 Newman LP, Bhat N, Fleming JA, Neuzil KM. 2018. Global influenza seasonality to inform country-level vaccine programs: an analysis of WHO FluNet influenza surveillance data between 2011 and 2016. *PLoS ONE*. 13(2):e0193263. doi:10.1371/journal.pone.0193263

10 Saha S, *et al.* 2014. Influenza seasonality and vaccination timing in tropical and subtropical areas of southern and south-eastern Asia. *Bull World Health Organ*. 92(5):318–330.

11 Viboud C, Alonso WJ, Simonsen L. 2006. Influenza in tropical regions. *PLoS Med*. 3(4):e89. doi:10.1371/journal.pmed.0030089

12 Brooks WA, *et al.* 2010. Influenza is a major contributor to childhood pneumonia in a tropical developing country. *Pediatr Infect Dis J*. 29(3):216–221.

13 Li Y, *et al.* 2019. Global patterns in monthly activity of influenza virus, respiratory syncytial virus, parainfluenza virus, and metapneumovirus: a systematic analysis. *Lancet Glob Health*. 7(8):e1031–e1045.

14 Shaman J, Pitzer VE, Viboud C, Grenfell BT, Lipsitch M. 2010. Absolute humidity and the seasonal onset of influenza in the continental United States. *PLoS Biol*. 8(2):e1000316. doi:10.1371/journal.pbio.1000316

15 Lowen AC, Mubareka S, Steel J, Palese P. 2007. Influenza virus transmission is dependent on relative humidity and temperature. *PLoS Pathog*. 3(10):e151. doi:10.1371/journal.ppat.0030151

16 Rao BL, Banerjee K. 1993. Influenza surveillance in Pune, India, 1978–1990. *Bull World Health Organ*. 71(2):177–181.

17 Tamerius JD, *et al.* 2013. Environmental predictors of seasonal influenza epidemics across temperate and tropical climates. *PLoS Pathog*. 9(3):e1003194. doi:10.1371/journal.ppat.1003194

18 Deyle ER, Maher MC, Hernandez RD, Basu S, Sugihara G. 2016. Global environmental drivers of influenza. *Proc Natl Acad Sci USA*. 113(46):13081–13086. doi:10.1073/pnas.1607747113

19 Yuan H, Kramer SC, Lau EHY, Cowling BJ, Yang W. 2021. Modeling influenza seasonality in the tropics and subtropics. *PLoS Comput Biol*. 17(6):e1009050. doi:10.1371/journal.pcbi.1009050

20 Tamerius J, *et al.* 2011. Global influenza seasonality: reconciling patterns across temperate and tropical regions. *Environ Health Perspect*. 119(4):439–445. doi:full/10.1289/ehp.1002383

21 Zaman RU, *et al.* 2009. Influenza in outpatient ILI case-patients in national hospital-based surveillance, Bangladesh, 2007–2008. *PLoS ONE*. 4(12):e8452. doi:10.1371/journal.pone.0008452

22 Berry I, *et al.* 2022 Aug. Seasonality of influenza and coseasonality with avian influenza in Bangladesh, 2010–2019: a retrospective, time-series analysis. *Lancet Glob Health*. 10(8):e1150–e1158.

23 Marinović AB, Swaan C, Steenbergen Jv, Kretzschmar M. 2015. Quantifying reporting timeliness to improve outbreak control. *Emerging Infect Dis*. 21(2):209–216.

24 Dalziel BD, *et al.* 2018. Urbanization and humidity shape the intensity of influenza epidemics in US cities. *Science*. 362(6410):75–79.

25 Lowen AC, Steel J, Mubareka S, Palese P. 2008. High temperature (30°C) blocks aerosol but not contact transmission of influenza virus. *J Virol*. 82(11):5650–5652. doi:10.1128/JVI.00325-08

26 Imai C, *et al.* 2014. Tropical influenza and weather variability among children in an urban low-income population in Bangladesh. *Glob Health Action*. 7:24413.

27 Merced-Morales A, *et al.* 2022. Influenza activity and composition of the 2022–2023 influenza vaccine—United States, 2021–2022 season. *Morb Mortal Wkly Rep*. 71(29):913–919.

28 Martinez PP, Li J, Cortes CP, Baker RE, Mahmud AS. 2022. The return of wintertime respiratory virus outbreaks and shifts in the age structure of incidence in the southern hemisphere. *Open Forum Infect Dis*. 9(12):ofac650. doi:10.1093/ofid/ofac650

29 Yang W, *et al.* 2018. Dynamics of influenza in tropical Africa: temperature, humidity, and co-circulating (sub)types. *Influenza Other Respir Viruses*. 12(4):446–456. doi:10.1111/irv.12556

30 Engebretsen S, *et al.* 2020. Time-aggregated mobile phone mobility data are sufficient for modelling influenza spread: the case of Bangladesh. *J R Soc Interface*. 17(167):20190809.

31 Mahmud AS, *et al.* 2021. Megacities as drivers of national outbreaks: the 2017 chikungunya outbreak in Dhaka, Bangladesh. *PLoS Negl Trop Dis*. 15(2):e0009106. doi:10.1371/journal.pntd.0009106

32 Grenfell BT, Bjørnstad ON, Finkenstädt BF. 2002. Dynamics of measles epidemics: scaling noise, determinism, and predictability with the TSIR model. *Ecol Monogr*. 72(2):185–202.

33 Akhtar Z, *et al.* 2021. Seasonal influenza during the COVID-19 pandemic in Bangladesh. *PLoS ONE*. 16(8):e0255646.

34 Hersbach H, *et al.* 2020. The ERA5 global reanalysis. *Q J R Meteorol Soc*. 146(730):1999–2049. doi:10.1002/qj.3803

35 Harris I, Osborn TJ, Jones P, Lister D. 2020. Version 4 of the CRU TS monthly high-resolution gridded multivariate climate dataset. *Sci Data*. 7(1):109. doi:10.1038/s41597-020-0453-3

36 Dunne JP, *et al.* 2020. The GFDL earth system model version 4.1 (GFDL-ESM 4.1): overall coupled model description and simulation characteristics. *J Adv Model Earth Syst*. 12(11):e2019MS002015. doi:10.1029/2019MS002015

37 Finkenstädt BF, Grenfell BT. 2000. Time series modelling of childhood diseases: a dynamical systems approach. *J R Stat Soc C (Appl Stat)*. 49(2):187–205. doi:10.1111/1467-9876.00187